Signals of doubly-charged Higgsinos at the CERN Large Hadron Collider

Durmuş A. Demir,[1,2] Mariana Frank,[3] Katri Huitu,[4] Santosh Kumar Rai,[4] and Ismail Turan[3]

[1]*Department of Physics, Izmir Institute of Technology, IZTECH, TR35430 Izmir, Turkey*

[2]*Deutsches Elektronen—Synchrotron, DESY, D-22603 Hamburg, Germany*

[3]*Department of Physics, Concordia University, 7141 Sherbrooke Street West, Montreal, Quebec H4B 1R6, Canada*

[4]*Department of Physics, University of Helsinki and Helsinki Institute of Physics, P.O. Box 64, FIN-00014 Helsinki, Finland*

(Received 30 May 2008; published 28 August 2008)

Several supersymmetric models with extended gauge structures, motivated by either grand unification or by neutrino mass generation, predict light doubly-charged Higgsinos. In this work we study productions and decays of doubly-charged Higgsinos present in left-right supersymmetric models, and show that they invariably lead to novel collider signals not found in the minimal supersymmetric model or in any of its extensions motivated by the μ problem or even in extra dimensional theories. We investigate their distinctive signatures at the Large Hadron Collider in both pair- and single-production modes, and show that they are powerful tools in determining the underlying model via the measurements at the Large Hadron Collider experiments.

DOI: 10.1103/PhysRevD.78.035013 PACS numbers: 12.60.Jv, 12.60.Fr

I. INTRODUCTION

The Large Hadron Collider (LHC), the highest energy collider ever built, starts operating this year, and will provide a clean window into ''new physics'' at the TeV scale. The ''new physics'' scenarios, designed to solve the gauge hierarchy problem, generally bring about new particles and interaction schemes. Supersymmetric theories (SUSY), for instance, provide an elegant solution to the gauge hierarchy problem by doubling the particle spectrum of the standard model, and their gauge sector could be minimal as in the minimal supersymmetric model (MSSM) or nonminimal as in models with extended gauge structures. Experiments at the LHC will be probing these new particles as well as new interaction laws among them.

A general, although not universally present, feature of SUSY, is that, if R parity $R = (-1)^{(3B+L+2S)}$ (with B, L, and S being baryon, lepton, and spin quantum numbers, respectively) is conserved, the absolute stability of the lightest supersymmetric partner (LSP) is guaranteed. This state qualifies to be a viable candidate for cold dark matter in the Universe (see, for instance, [1] and references therein). Supersymmetric models provide a viable dark matter candidate in the lightest neutral fermion composed of neutral gauginos and Higgsinos. In general, decays of all supersymmetric partners necessarily end with the LSP, and given its absolute stability, it leaves any particle detector undetected, and thus, appears as a ''momentum imbalance'' or ''missing energy'' in collider processes, including the ones at the LHC [2]. In this sense, all scattering processes involving the superpartners are inherently endowed with incomplete final states.

Though supersymmetry, as an organizing principle, resolves the gauge hierarchy problem, there is no unique supersymmetric field theory to model ''new physics'' at the TeV scale. Indeed, MSSM, though it stands as the minimal supersymmetric model directly constructed from the standard model (SM) spectrum, suffers from the well-known μ problem and lacks a natural understanding of neutrino masses in the absence of right-handed neutrinos (which must be either ultraheavy to facilitate the seesaw mechanism or must possess naturally suppressed Yukawa couplings to left-handed ones). These features generally require a nontrivial extension of the MSSM which typically involves additional gauge structures. Indeed, low-energy models following from supersymmetric grand unified theories or strings [3] generally predict either extension of the SM gauge group by some extra gauge factors, such as a number of extra $U(1)$ symmetries, or embedment of the SM gauge group into larger gauge groups. Concerning the latter, one can consider several structures, for instance, the left-right symmetric SUSY (LRSUSY) gauge theory $SU(3)_C \times SU(2)_L \times SU(2)_R \times U(1)_{B-L}$. In general, models of ''new physics'' (in terms of their gauge and Higgs sectors) are distinguished by certain characteristic signatures in regard to their lepton and jet spectra of the final state. In this work, we investigate signatures specific to LRSUSY and compare with those of the MSSM wherever appropriate. LRSUSY presents an attractive alternative/generalization of the MSSM [4,5]. It can be viewed as an alternative to the MSSM by itself or as a covering structure of the MSSM following from supersymmetric grand unified theories or strings, such as $SO(10)$. LRSUSY models disallow explicit R-parity breaking in the Lagrangian, thus predicting naturally a supersymmetric dark matter candidate [1]. They provide a solution to the strong and weak CP problems present in the MSSM [6]. If one chooses Higgs triplet fields, with quantum numbers $B - L = \pm 2$, to break the $SU(2)_R$ gauge group, the neutrino masses turn out to be induced by the seesaw mechanism [7]. The fermionic partners of

the Higgs triplet bosons are specific to the supersymmetric version, and some of them carry double charge and two units of L number, making them perfect testing/searching grounds for exotics. It has been shown that, if the scale for left-right symmetry breaking is chosen so that the light neutrinos have the experimentally expected masses, these doubly-charged Higgsinos can be light, with masses in the range of $\mathcal{O}(100)$ GeV [8–10]. Such particles could be produced in abundance at the LHC and thus give definite identifiable signatures of left-right symmetry. The doubly-charged Higgsinos have been studied in some detail in Refs. [11–13], where the production of Higgsinos at linear colliders was analyzed. The doubly-charged Higgsinos can also appear in the so-called 3-3-1 models (models based on the $SU(3)_c \times SU(3)_L \times U(1)_N$ symmetry) [14].

In this work, we study doubly-charged Higgsinos at the CERN Large Hadron Collider (LHC), produced singly or in pairs, via various leptonic final states. We focus on three benchmark points of the model and analyze the LHC signals resulting from the decays of the doubly-charged Higgsinos. In order to obtain definitive predictions for the signal, we perform the analysis in the context of the LRSUSY model, though we expect the results for the 3-3-1 model to be similar. The paper is organized as follows: In Sec. II we present a brief introduction to the model for completeness and clarification of the notation. In Sec. III we focus on the details and characteristics of the production cross sections of the doubly-charged Higgsinos, and discuss their possible decay channels (either through two-body or three-body, depending on the spectrum characteristics) proceeding with charged states. Herein we analyze single- and pair-production modes separately. Finally, in Sec. IV we conclude and discuss the significance of the results in regard to measurements at the LHC.

II. THE LEFT-RIGHT SUPERSYMMETRIC MODEL

In this section, we review briefly the relevant features of the model necessary for the analysis which follows in the later sections. For a more detailed information about the model see, for instance, [4,5]. The chiral matter in LRSUSY consist of three families of quark and lepton superfields

$$Q = \begin{pmatrix} u \\ d \end{pmatrix} \sim \left(3, 2, 1, \frac{1}{3}\right), \quad Q^c = \begin{pmatrix} d^c \\ u^c \end{pmatrix} \sim \left(3^*, 1, 2, -\frac{1}{3}\right),$$
$$L = \begin{pmatrix} \nu \\ e \end{pmatrix} \sim (1, 2, 1, -1), \quad L^c = \begin{pmatrix} e^c \\ \nu^c \end{pmatrix} \sim (1, 1, 2, 1),$$

where the numbers in the brackets denote the quantum numbers under $SU(3)_C \times SU(2)_L \times SU(2)_R \times U(1)_{B-L}$ gauge factors.

The symmetry breaking is achieved by a Higgs sector consisting of bidoublet and triplet Higgs superfields. The choice of the triplet Higgs fields has the advantage that it facilitates the seesaw mechanism for neutrino masses with renormalizable couplings. Here are the decompositions of the Higgs superfields

$$\begin{aligned}
\Phi_1 &= \begin{pmatrix} \Phi_{11}^0 & \Phi_{11}^+ \\ \Phi_{12}^- & \Phi_{12}^0 \end{pmatrix} \sim (1, 2, 2, 0), \\
\Phi_2 &= \begin{pmatrix} \Phi_{21}^0 & \Phi_{21}^+ \\ \Phi_{22}^- & \Phi_{22}^0 \end{pmatrix} \sim (1, 2, 2, 0), \\
\Delta_L &= \begin{pmatrix} \frac{1}{\sqrt{2}}\Delta_L^- & \Delta_L^0 \\ \Delta_L^{--} & -\frac{1}{\sqrt{2}}\Delta_L^- \end{pmatrix} \sim (1, 3, 1, -2), \\
\delta_L &= \begin{pmatrix} \frac{1}{\sqrt{2}}\delta_L^+ & \delta_L^{++} \\ \delta_L^0 & -\frac{1}{\sqrt{2}}\delta_L^+ \end{pmatrix} \sim (1, 3, 1, 2), \\
\Delta_R &= \begin{pmatrix} \frac{1}{\sqrt{2}}\Delta_R^- & \Delta_R^0 \\ \Delta_R^{--} & -\frac{1}{\sqrt{2}}\Delta_R^- \end{pmatrix} \sim (1, 1, 3, -2), \\
\delta_R &= \begin{pmatrix} \frac{1}{\sqrt{2}}\delta_R^+ & \delta_R^{++} \\ \delta_R^0 & -\frac{1}{\sqrt{2}}\delta_R^+ \end{pmatrix} \sim (1, 1, 3, 2),
\end{aligned} \tag{1}$$

where numbers in the brackets again denote the quantum numbers of fields under $SU(3)_C \times SU(2)_L \times SU(2)_R \times U(1)_{B-L}$.

The superpotential of the model is given by

$$\begin{aligned}
W = {} & \mathbf{Y}_Q^{(i)} Q^T \Phi_i i\tau_2 Q^c + \mathbf{Y}_L^{(i)} L^T \Phi_i i\tau_2 L^c + i(\mathbf{h}_{ll} L^T \tau_2 \delta_L L \\
& + \mathbf{h}_{ll} L^{cT} \tau_2 \Delta_R L^c) + \mu_3 \,\mathrm{Tr}[\Delta_L \delta_L + \Delta_R \delta_R] \\
& + \mu_{ij} \,\mathrm{Tr}[i\tau_2 \Phi_i^T i\tau_2 \Phi_j] + W_{\mathrm{NR}},
\end{aligned} \tag{2}$$

where W_{NR} denotes (possible) nonrenormalizable terms arising from integrating out of the heavier fields. The Lagrangian of the model, as usual, consists of the standard F-terms, D-terms as well as the soft SUSY-breaking terms. Considering the decay and production processes under investigation, the relevant parts of the soft-breaking Lagrangian read as

$$\begin{aligned}
-L_{\mathrm{soft}} = {} & (m_\Phi^2)_{ij} \Phi_i^\dagger \Phi_j + (m_L^2)_{ij} \tilde{l}_{Li}^\dagger \tilde{l}_{Lj} + (m_R^2)_{ij} \tilde{l}_{Ri}^\dagger \tilde{l}_{Rj} \\
& + [\mathbf{A}_L^i \mathbf{Y}_L^{(i)} \tilde{L}^T \Phi_i i\tau_2 \tilde{L}^c + i\mathbf{A}_{LR} \mathbf{h}_{ll} (\tilde{L}^T \tau_2 \delta_L \tilde{L} \\
& + \tilde{L}^{cT} \tau_2 \Delta_R \tilde{L}^c) + \mathrm{H.c.}] - [m_{LR}^2 \,\mathrm{Tr}[\Delta_R \delta_R \\
& + \Delta_L \delta_L] - [B\mu_{ij} \Phi_i \Phi_j + \mathrm{H.c.}]
\end{aligned} \tag{3}$$

where the first line stands for mass-squared terms, the second and third for trilinear couplings [holomorphically corresponding to similar terms in (2)], and the last two for bilinear couplings.

Combining (3) with F-term and D-term contributions, minimization of the Higgs potential gives vacuum expectation values (VEVs) for the neutral components of the Higgs fields in (1), as discussed in detail in [1,13].

In the following, we give a detailed discussion of the charged and neutral fermions as well as sleptons in LRSUSY in preparation for a thorough analysis of the productions and decays of the doubly-charged Higgsinos.

A. Charginos

As follows from the decompositions of the Higgs fields in (1), the particle spectrum consists of doubly-charged Higgsinos $\tilde{\Delta}_L^{--}$, $\tilde{\delta}_L^{++}$, $\tilde{\Delta}_R^{--}$ and $\tilde{\delta}_R^{++}$. In the Lagrangian basis they possess the bilinear terms

$$\mathcal{L}_{\tilde{\Delta}} = -M_{\tilde{\Delta}^{--}}\tilde{\Delta}_L^{--}\tilde{\delta}_L^{++} - M_{\tilde{\Delta}_R^{--}}\tilde{\Delta}_R^{--}\tilde{\delta}_R^{++} + \text{H.c.}, \quad (4)$$

where the Higgsino mass $M_{\tilde{\Delta}^{--}} \equiv \mu_3$ in the notation of (2). In addition to these doubly-charged ones, the model consists also of a total of six singly-charged Higgsinos and gauginos, corresponding to λ_L, λ_R, $\tilde{\phi}_u$, $\tilde{\phi}_d$, $\tilde{\Delta}_L^-$, $\tilde{\delta}_L^+$, $\tilde{\delta}_R^+$, and $\tilde{\Delta}_R^-$. The bilinears in these charged states combine to give

$$\mathcal{L}_C = -\frac{1}{2}(\psi^{+T}, \psi^{-T})\begin{pmatrix} 0 & X^T \\ X & 0 \end{pmatrix}\begin{pmatrix} \psi^+ \\ \psi^- \end{pmatrix} + \text{H.c.}, \quad (5)$$

where $\psi^{+T} = (-i\lambda_L^+, -i\lambda_R^+, \tilde{\phi}_{1d}^+, \tilde{\phi}_{1u}^+, \tilde{\delta}_L^+, \tilde{\delta}_R^+)$, $\psi^{-T} = (-i\lambda_L^-, -i\lambda_R^-, \tilde{\phi}_{2d}^-, \tilde{\phi}_{2u}^-, \tilde{\Delta}_L^-, \tilde{\Delta}_R^-)$, and

$$X = \begin{pmatrix} M_L & 0 & 0 & g_L\kappa_d & \sqrt{2}g_L v_{\delta_L} & 0 \\ 0 & M_R & 0 & g_R\kappa_d & 0 & \sqrt{2}g_R v_{\delta_R} \\ g_L\kappa_u & g_R\kappa_u & 0 & -\mu_1 & 0 & 0 \\ 0 & 0 & -\mu_1 & 0 & 0 & 0 \\ \sqrt{2}g_L v_{\Delta_L} & 0 & 0 & 0 & -\mu_3 & 0 \\ 0 & \sqrt{2}g_R v_{\Delta_R} & 0 & 0 & 0 & -\mu_3 \end{pmatrix}$$

in the mass mixing matrix. We have set, for simplicity, $\mu_{ij} \equiv \mu_1$ for all $(i \neq j)$. Here $\kappa_u = \langle\Phi_{11}^0\rangle$, $\kappa_d = \langle\Phi_{22}^0\rangle$, $v_{\Delta_{L,R}} = \langle\Delta_{L,R}^0\rangle$, $v_{\delta_{L,R}} = \langle\delta_{L,R}^0\rangle$, and $M_{L,R}$ are the $SU(2)_{L,R}$ gaugino masses, respectively. The physical chargino states $\tilde{\chi}_i$ are obtained by

$$\tilde{\chi}_i^+ = V_{ij}\psi_j^+, \qquad \tilde{\chi}_i^- = U_{ij}\psi_j^- \qquad (i,j = 1,\ldots 6), \quad (6)$$

with V and U unitary matrices satisfying

$$U^* X V^{-1} = M_D \quad (7)$$

where M_D is a 6×6 diagonal matrix with non-negative entries. The mixing matrices U and V are obtained by computing the eigensystem of $XX^\dagger$ and $X^\dagger X$, respectively.

While κ_u and κ_d are the VEVs responsible for giving masses to quarks and leptons, the non-MSSM Higgs VEVs, v_{δ_L} and v_{Δ_R} are responsible for neutrino masses. v_{Δ_L} and v_{δ_L} enter in the formula for the mass of W_L (or the ρ parameter), while v_{Δ_R}, v_{δ_R} enter in the formula for the mass of W_R. It is thus justified to take v_{Δ_L}, v_{δ_L} to be negligibly small. For v_{Δ_R} there are two possibilities: either v_{Δ_R} is $\approx 10^{13}$ GeV [8,15], which supports the seesaw mechanism, leptogenesis and provides masses for the light neutrinos in agreement with experimental constraints, but offers no hope to see right-handed particles; or v_{Δ_R} is $\approx$ 1–10 TeV, but one must introduce something else (generally an intermediate scale, or an extra symmetry) to make the neutrinos light [8,9,16].

B. Neutralinos

In LRSUSY there are 11 neutral fermions, corresponding to λ_Z, $\lambda_{Z'}$, λ_{B-L}, $\tilde{\phi}_{1u}^0$, $\tilde{\phi}_{2u}^0$, $\tilde{\phi}_{1d}^0$, $\tilde{\phi}_{2d}^0$, $\tilde{\Delta}_L^0$, $\tilde{\Delta}_R^0$, $\tilde{\delta}_L^0$, and $\tilde{\delta}_R^0$. Their bilinears give the contribution to the Lagrangian

$$\mathcal{L}_N = -\frac{1}{2}\psi^{0T} Z \psi^0 + \text{H.c.}, \quad (8)$$

where $\psi^0 = (-i\lambda_L^0, -i\lambda_R^0, -i\lambda_{B-L}, \tilde{\phi}_{1u}^0, \tilde{\phi}_{2d}^0, \tilde{\Delta}_L^0, \tilde{\delta}_L^0, \tilde{\Delta}_R^0, \tilde{\delta}_R^0, \tilde{\phi}_{1d}^0, \tilde{\phi}_{2u}^0)^T$, and the mass mixing matrix Z is given by

$$Z = \begin{pmatrix} M_L & 0 & 0 & -\frac{g_L\kappa_u}{\sqrt{2}} & \frac{g_L\kappa_d}{\sqrt{2}} & -2^{1/2}g_L v_{\Delta_L} & -2^{1/2}g_L v_{\delta_L} & 0 & 0 & 0 & 0 \\ 0 & M_R & 0 & \frac{g_L\kappa_u}{\sqrt{2}} & \frac{g_L\kappa_d}{\sqrt{2}} & 0 & 0 & -2^{1/2}g_R v_{\Delta_R} & -2^{1/2}g_R v_{\delta_R} & 0 & 0 \\ 0 & 0 & M_{B-L} & 0 & 0 & 2^{3/2}g_V v_{\Delta_L} & 2^{3/2}g_V v_{\delta_L} & 2^{3/2}g_V v_{\Delta_R} & 2^{3/2}g_V v_{\delta_R} & 0 & 0 \\ -\frac{g_L\kappa_u}{\sqrt{2}} & \frac{g_R\kappa_u}{\sqrt{2}} & 0 & 0 & \mu_1 & 0 & 0 & 0 & 0 & 0 & 0 \\ \frac{g_L\kappa_d}{\sqrt{2}} & -\frac{g_R\kappa_d}{\sqrt{2}} & 0 & \mu_1 & 0 & 0 & 0 & 0 & 0 & 0 & 0 \\ -2^{1/2}g_L v_{\Delta_L} & 0 & 2^{3/2}g_V v_{\Delta_L} & 0 & 0 & 0 & -\mu_3 & 0 & 0 & 0 & 0 \\ -2^{1/2}g_L v_{\delta_L} & 0 & 2^{3/2}g_V v_{\delta_L} & 0 & 0 & -\mu_3 & 0 & 0 & 0 & 0 & 0 \\ 0 & -2^{1/2}g_R v_{\Delta_R} & 2^{3/2}g_V v_{\Delta_R} & 0 & 0 & 0 & 0 & 0 & -\mu_3 & 0 & 0 \\ 0 & -2^{1/2}g_R v_{\delta_R} & 2^{3/2}g_V v_{\delta_R} & 0 & 0 & 0 & 0 & -\mu_3 & 0 & 0 & 0 \\ 0 & 0 & 0 & 0 & 0 & 0 & 0 & 0 & 0 & 0 & \mu_1 \\ 0 & 0 & 0 & 0 & 0 & 0 & 0 & 0 & 0 & \mu_1 & 0 \end{pmatrix} \quad (9)$$

with M_{B-L} being the $U(1)_{B-L}$ gaugino mass. The physical neutralinos are defined via

$$\tilde{\chi}_i^0 = N_{ij}\psi_j^0 \qquad (i, j = 1, 2, \ldots 11), \tag{10}$$

where N is the unitary matrix that diagonalizes Z

$$N^* Z N^T = Z_D, \tag{11}$$

with Z_D being an 11×11 diagonal matrix with non-negative entries. The lightest of the 11 neutralinos, $\tilde{\chi}_1^0$, is a candidate for cold dark matter in the Universe [1].

C. Scalar leptons

Combining F-term, D-term, and soft-breaking contributions pertaining to sleptons, their mass-squared matrix is found to be

$$\mathcal{M}_L^2 = \begin{pmatrix} M_{LL}^2 & M_{LR}^2 \\ M_{RL}^2 & M_{RR}^2 \end{pmatrix} \tag{12}$$

where

$$\begin{aligned} M_{LL}^2 &= m_L^2 + m_\ell^2 + m_Z^2(T_{3\ell} + \sin^2\theta_W)\cos 2\beta, \\ M_{LR}^2 &= M_{RL}^{2\dagger} = m_\ell(A + \mu \tan\beta), \\ M_{RR}^2 &= m_R^2 + m_\ell^2 - m_Z^2 \sin^2\theta_W \cos 2\beta \end{aligned} \tag{13}$$

as follows from (3) with $\ell = e,\ \mu,\ \tau$. We neglect intergenerational mixings, and intragenerational left-right mixing can be important only for $\ell = \tau$ flavor.

III. PRODUCTION AND DECAY OF DOUBLY-CHARGED HIGGSINOS

Having described neutralino, chargino, and slepton sectors in detail, we now analyze productions and decays of doubly-charged Higgsinos. The relevant Feynman rules are listed in the appendix. The pair-production processes at the LHC involve

(i) $pp \longrightarrow \tilde{\Delta}^{++}\tilde{\Delta}^{--}$ (illustrated in Fig. 1) which proceeds with s-channel γ and $Z_{L,R}$ exchanges, and

(ii) $pp \longrightarrow \tilde{\chi}_1^+\tilde{\Delta}^{--}$ (illustrated in Fig. 2)

which rests on s-channel $W_{L,R}$ exchanges. Both processes are generated by quark-antiquark annihilation at the parton

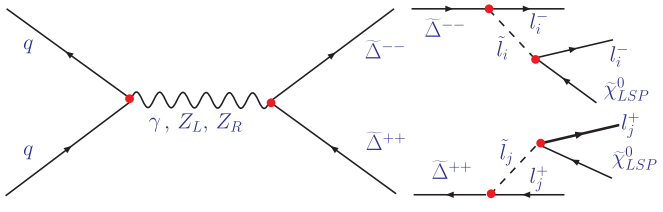

FIG. 1 (color online). Direct $\tilde{\Delta}^{--}$ pair production at the LHC. Subsequent decays of $\tilde{\Delta}^{--}$ give rise to two dileptons plus missing energy signal, if $M_{\tilde{l}_j} < M_{\tilde{\Delta}^{--}}$.

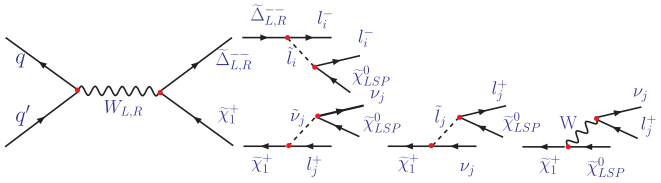

FIG. 2 (color online). Direct production of single $\tilde{\Delta}^{--}$ in association with $\tilde{\chi}_1^+$ at the LHC. Subsequent decays of $\tilde{\Delta}^{--}$ and $\tilde{\chi}_1^+$ give rise to a trilepton plus missing energy signal, if $M_{\tilde{\nu}_j} < M_{\tilde{\chi}_1^+}$ and $M_{\tilde{l}_j} < M_{\tilde{\Delta}^{--}}$.

level. The s-channel Higgs exchanges cannot give any significant contribution.

These doubly- and singly-charged fermions subsequently decay via a chain of cascades until the lightest neutralino χ_1^0 is reached. Given that charged leptons ($\ell = e$ and $\ell = \mu$, especially) give rise to rather clean signals at the ATLAS and CMS detectors, we classify final states according to their lepton content in number, electric charge, and flavor. In general, the two-body decays of doubly-charged Higgsinos are given by

(i) $\tilde{\Delta}^{--} \longrightarrow \tilde{\ell}^-\ell^-$,
(ii) $\tilde{\Delta}^{--} \longrightarrow \Delta^{--}\tilde{\chi}_i^0$,
(iii) $\tilde{\Delta}^{--} \longrightarrow \tilde{\chi}_i^-\Delta^-$,
(iv) $\tilde{\Delta}^{--} \longrightarrow \tilde{\chi}_i^- W^-$,

whose decay products further cascade into lower-mass daughter particles of which leptons are of particular interest. The production and decay processes mentioned here are illustrated in Figs. 1 and 2. Clearly, pair-produced doubly-charged Higgsinos lead to $4\ell + \not{E}_T$ final states whereas single-produced doubly-charged Higgsinos give rise to $3\ell + \not{E}_T$ signals.

We assume that triplet Higgs bosons are heavier and degenerate in mass, which renders them kinematically inaccessible for the decay modes of the relatively lighter doubly-charged Higgsinos. The possibility of light observable doubly-charged Higgs bosons has been explored extensively in both phenomenological analyses [17] and experimental investigations [18] and is beyond the scope of this study. Therefore, we concentrate on the remaining accessible decay channels. For the numerical estimates we consider three sample points in the LRSUSY parameter space, as tabulated in Table I. A quick look at the resulting mass spectrum for the sparticles suggest that the chargino states are also heavier than or comparable to the doubly-charged Higgsinos, and hence, the favorable decay channel for $\tilde{\Delta}$ is $\tilde{\Delta}^{--} \longrightarrow \tilde{\ell}^-\ell^-$, provided that $m_{\tilde{l}} < M_{\tilde{\Delta}^{--}}$. For relatively light Higgsinos, one can, in principle, have $m_{\tilde{l}} > M_{\tilde{\Delta}^{--}}$ in which case the only allowed decay mode for the doubly-charged Higgsinos would be the 3-body decays, which would proceed dominantly through off shell sleptons: $\tilde{\Delta}^{--} \to \tilde{\ell}^{\star -}\ell^- \to \ell^-\ell^-\tilde{\chi}_1^0$. We have explicitly checked that the 3-body decay of the doubly-charged Higgsinos through the heavy off shell charginos or W

TABLE I. The numerical values assigned to the model parameters in defining the sample points **SPA**, **SPB**, and **SPC**. In each case, **S2** and **S3** designate parameter values which allow for **2**-body and **3**-body decays of doubly-charged Higgsinos, respectively. The VEVs of the left-handed Higgs triplets are taken as $v_{\Delta_L} \sim v_{\delta_L} \simeq 10^{-8}$ GeV. We assume the trilinear couplings A to be nonzero and set to 20 GeV. For the couplings we use $g_L = g_R = g$ and for $h_{ll} = 0.1$ [13].

	SPA		**SPB**		**SPC**	
Fields	$\tan\beta = 5$, $M_{B-L} = 25$ GeV		$\tan\beta = 5$, $M_{B-L} = 100$ GeV		$\tan\beta = 5$, $M_{B-L} = 0$ GeV	
	$M_L = M_R = 250$ GeV		$M_L = M_R = 500$ GeV		$M_L = M_R = 500$ GeV	
	$v_{\Delta_R} = 3000$ GeV, $v_{\delta_R} = 1000$ GeV		$v_{\Delta_R} = 2500$ GeV, $v_{\delta_R} = 1500$ GeV		$v_{\Delta_R} = 2500$ GeV, $v_{\delta_R} = 1500$ GeV	
	$\mu_1 = 1000$ GeV, $\mu_3 = 300$ GeV		$\mu_1 = 500$ GeV, $\mu_3 = 500$ GeV		$\mu_1 = 500$ GeV, $\mu_3 = 300$ GeV	
$\tilde{\chi}_i^0$ $(i = 1, 3)$	89.9, 180.6, 250.9 GeV		212.9, 441.2, 458.5 GeV		142.5, 265.6, 300.0 GeV	
$\tilde{\chi}_i^\pm$ $(i = 1, 3)$	250.9, 300.0, 953.9 GeV		459.4, 500.0, 500.0 GeV		300.0, 459.3, 500.0 GeV	
$M_{\tilde{\Delta}}$	300 GeV		500 GeV		300 GeV	
W_R, Z_R	2090.4, 3508.5 GeV		1927.2, 3234.8 GeV		1927.2, 3234.8 GeV	
	S2	**S3**	**S2**	**S3**	**S2**	**S3**
$m_{L,R}$	150 GeV	400 GeV	250 GeV	550 GeV	210 GeV	400 Gev
$(\tilde{e}_L, \tilde{e}_R)$	(156.9, 155.6 GeV),	(402, 402 GeV)	(254.2, 253.4 GeV),	(552, 552 GeV)	(214.9, 214.0 GeV),	(402.6, 402.2 GeV)
$(\tilde{\mu}_L, \tilde{\mu}_R)$	(156.9, 155.6 GeV),	(402, 402 GeV)	(254.2, 253.4 GeV),	(552, 552 GeV)	(214.9, 214.0 GeV),	(402.6, 402.2 GeV)
$(\tilde{\tau}_1, \tilde{\tau}_2)$	(155.4, 159.9 GeV),	(401, 406 GeV)	(252.5, 257.9 GeV),	(550, 556 GeV)	(550, 556 GeV)	(401.5, 403.3 GeV)

bosons is quite suppressed with respect to the two-body decay, and can be safely neglected.

We present our results for the Higgsino pair production for the two sample points **SPA** and **SPB** described in Table I. Since the cross sections for the single-production modes are highly suppressed for **SPA** and **SPB**, we consider yet another sample point, called **SPC** in Table I, which maximizes the single-production cross section of $\tilde{\Delta}_L^{--}$. It is also possible to find a sample point which maximizes the cross section for single $\tilde{\Delta}_R^{--}$ production. We discuss the single $\tilde{\Delta}_L^{--}$ production in detail and comment on the $\tilde{\Delta}_R^{--}$ case, as their features are fairly similar.

For the benchmark point in Table I, the doubly-charged Higgsinos assume the following 2- and 3-body decay branchings:

$$\begin{aligned} \mathrm{BR}(\tilde{\Delta}_{L/R}^{--} \to \tilde{\ell}_{iL/iR}^- \ell_i^-) &\simeq \frac{1}{3}, \qquad m_{\tilde{l}_i} < M_{\tilde{\Delta}^{--}} \\ \mathrm{BR}(\tilde{\ell}_{iL/iR}^- \to \ell_i^- \tilde{\chi}_1^0) &= 1, \\ \mathrm{BR}(\tilde{\Delta}_{L/R}^{--} \to \ell_i^- \ell_i^- \tilde{\chi}_1^0) &\simeq \frac{1}{3}, \qquad m_{\tilde{l}_i} > M_{\tilde{\Delta}^{--}} \end{aligned} \tag{14}$$

where $i = e, \mu, \tau$. One notes that only 3-body decay channel is allowed when $m_{\tilde{\ell}_i} > M_{\tilde{\Delta}}$. (We discuss the chargino decay later for the single-production mode). To fix our notations, we denote by **S2** the signal corresponding to the **2**-body decay of $\tilde{\Delta}$ and by **S3** the signal corresponding to the **3**-body decay of $\tilde{\Delta}$. The two separate cases correspond to two different choices of the slepton masses for the same sample point. These features are shown in parentheses as columns in Table I for **SPA**, **SPB** and **SPC**.

In what follows we shall analyze single- and pair-productions of doubly-charged Higgsinos separately by using Monte Carlos techniques.

A. Pair-production of doubly-charged Higgsinos

The pair-production of doubly-charged Higgsinos at the LHC occurs through the s-channel exchanges of the neutral gauge bosons in the model, as depicted in Fig. 1. The heavy Z boson (Z_R) can enhance the production cross section through resonance effect, if kinematically accessible at the LHC. In Fig. 3 we plot production cross sections for $\tilde{\Delta}^{--}$

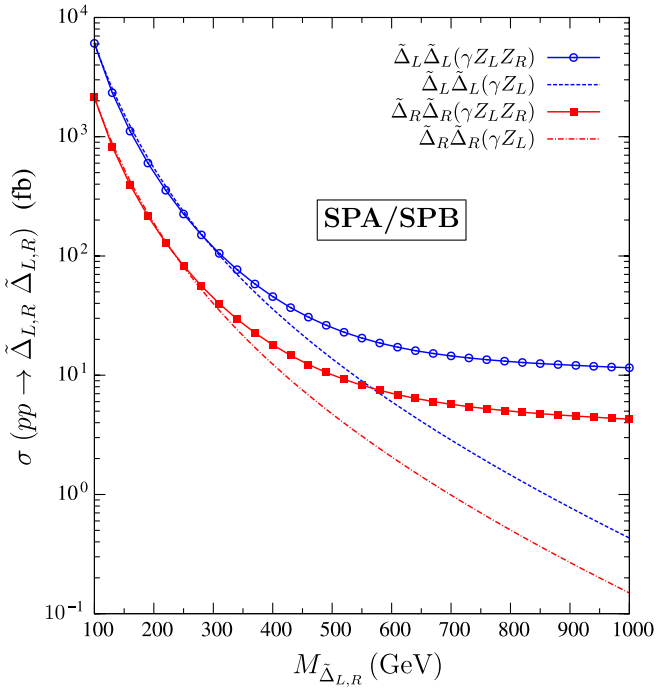

FIG. 3 (color online). The pair-production cross sections for doubly-charged Higgsinos in LRSUSY at the LHC. The plots are performed by using the parameter sets **SPA**/**SPB** except that $M_{\tilde{\Delta}^{--}} \equiv \mu_3$ is allowed to vary from 100 GeV up to 1 TeV. See the text for explanation of curves.

chiralities and exchange gauge bosons. It is seen that the cross section is quite sizeable for sufficiently light doubly-charged Higgsinos: it starts at $\sim 10^4$ fb at $M_{\tilde{\Delta}} \simeq 100$ GeV and stays above ~ 10 fb even if $M_{\tilde{\Delta}}$ is stretched up to 1 TeV provided that contributions of all three neutral gauge bosons, γ, Z_L, and Z_R, are included. The figure also shows that cross sections, for both chiralities, fall rapidly with increasing $M_{\tilde{\Delta}}$ if Z_R gauge boson is decoupled from the low-energy spectrum. The plots highlight the fact that the heavy Z_R contribution becomes more significant for the pair production of heavier states, as seen in Fig. 3. Pair production of heavier states requires a much higher effective center of mass energy $\sqrt{\hat{s}} = \sqrt{x_1 x_2 s}$, where x_i's are the momentum fractions carried by the partons at the hadron collider. This would yield a stronger s-channel suppression of the SM contributions coming from the photon and Z exchange and enhance the contribution coming from the heavy Z_R exchange.

The doubly-charged Higgsinos decay according to Eq. (14) into two same-sign same-flavor (SSSF) leptons and the lightest neutralino $\tilde{\chi}_1^0$, the LSP. This decay pattern gives rise to final states involving four isolated leptons of the form $(\ell_i^- \ell_i^-)(\ell_j^+ \ell_j^+)$ where ℓ_i and ℓ_j are not necessarily identical lepton flavors. More precisely, final states generated by the decays of doubly-charged Higgsino pairs generally contain tetraleptons plus missing momentum carried away by the LSP

$$pp \to \tilde{\Delta}^{++}\tilde{\Delta}^{--} \to (\ell_i^+ \ell_i^+) + (\ell_j^- \ell_j^-) + \not{E}_T, \qquad (15)$$

where $\ell_i, \ell_j = e, \mu, \tau$.

The $4\ell + \not{E}_T$ signal receives contributions from the pair-production of both chiral states of the doubly-charged Higgsino. Since at the LHC it is difficult to determine chiralities of particles, it is necessary to add up their individual contributions to obtain the total number of events. This yields a rather clean and robust $4l+$ missing p_T signal at the LHC with highly suppressed SM background. In fact, one finds that the SM background with tetraleptons, where $\ell_i = e$ and $\ell_j = \mu$ in Eq. (15) with large missing transverse energy ($\not{E}_T \geq 50$ GeV), is very suppressed ($\mathcal{O} \sim 10^{-3}$ fb) and can therefore be safely neglected compared to the signal generated by doubly-charged Higgsino pairs. This fact makes this channel highly promising for an efficient and clean disentanglement of LRSUSY effects.

For triggering and enhancing the $4\ell + \not{E}_T$ signal we impose the following kinematic cuts:

(i) The charged leptons in the final state must respect the rapidity cut $|\eta_\ell| < 2.5$.
(ii) The charged leptons in the final state must have a transverse momentum $p_T > 25$ GeV.
(iii) To ensure proper resolution between the final-state leptons we demand $\Delta R_{\ell\ell} > 0.4$ for each pair of leptons, where $\Delta R = \sqrt{(\Delta\phi)^2 + (\Delta\eta)^2}$, ϕ being the azimuthal angle.
(iv) The missing transverse energy must be $\not{E}_T > 50$ GeV.
(v) The pairs of oppositely-charged leptons of the same flavor have at least 10 GeV invariant mass.

For numerical analysis, we have included the LRSUSY model into CALCHEP 2.4.5 [19] and generated the event files for the production and decays of the doubly-charged Higgsinos using the CALCHEP event generator. The event files are then passed through the CALCHEP-PYTHIA interface where we include the effects of both initial and final state radiations using PYTHIA switches [20] to smear the final states. We use the leading order CTEQ6L [21] parton distribution functions (PDF) for the quarks in protons.

Below we list production cross sections as well as total event cross sections (after applying the kinematic cuts mentioned above). For four-lepton plus missing energy signal we take specifically the $2\mu^- + 2e^+ + \not{E}_T$ final state, and find the following results for **SPA** and **SPB**:

(1) **SPA**:

$$\sigma(\tilde{\Delta}_L^{--}\tilde{\Delta}_L^{++}) = 117.9 \text{ fb}$$

and

$$\sigma(\tilde{\Delta}_R^{--}\tilde{\Delta}_R^{++}) = 44.5 \text{ fb}.$$

After imposing the kinematic cuts, the total cross section for the final state (summing over contributions coming from doubly-charged Higgsinos of either chirality) turns out to be:

(a) **S2** $\sigma(2\mu^- 2e^+ + \not{E}_T) = 7.71$ fb,
(b) **S3** $\sigma(2\mu^- 2e^+ + \not{E}_T) = 7.02$ fb
(c) **SPB**:

$$\sigma(\tilde{\Delta}_L^{--}\tilde{\Delta}_L^{++}) = 32.4 \text{ fb}$$

and

$$\sigma(\tilde{\Delta}_R^{--}\tilde{\Delta}_R^{++}) = 12.95 \text{ fb}.$$

After applying the kinematic cuts we find:

(a) **S2** $\sigma(2\mu^- 2e^+ + \not{E}_T) = 2.43$ fb,
(b) **S3** $\sigma(2\mu^- 2e^+ + \not{E}_T) = 2.66$ fb.

The same numerical results hold also when the final state is charge-conjugated, i.e. $2\mu^+ 2e^- + \not{E}_T$. In principle, one can also work with final states where one of the lepton flavors is τ. Then one needs to fold in the efficiencies for τ identification at LHC with the above numbers to get the correct event rates.

In Fig. 4 we plot the binwise distribution of the spatial resolution between the charged lepton pairs for the different cases indicated on the curves. We choose to use the events for the case **S2** for both **SPA** and **SPB**, as the characteristic features of the distributions remain the same for **S3**. Here the notation $l^\pm l^\pm$ stands for $\mu^-\mu^-$ or e^+e^+. The figure manifestly shows the difference between

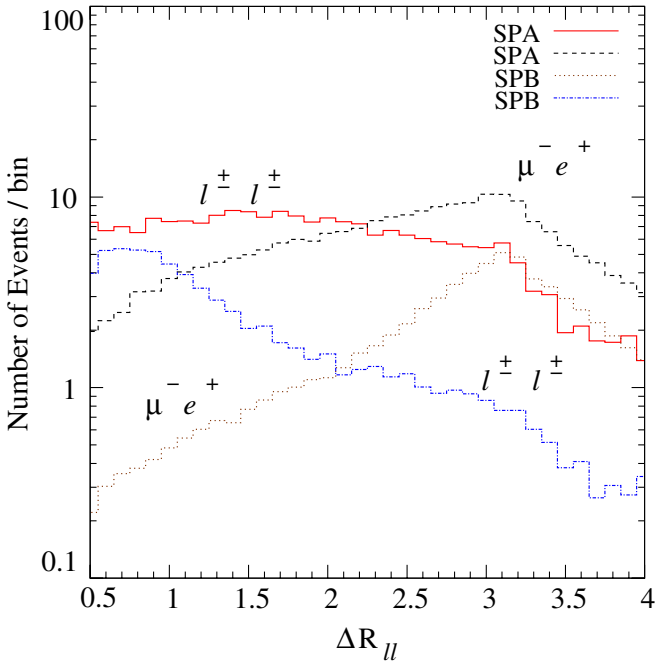

FIG. 4 (color online). Binwise distribution of ΔR with binsize 0.1 and integrated luminosity of $\int \mathcal{L} dt = 30$ fb^{-1}.

the SSSF leptons whose distributions are peaked at low values of ΔR and the opposite-sign different-flavor (OSDF) leptons whose distributions maximize at higher values of ΔR. The SSSF leptons originate from the cascade decay of one single doubly-charged Higgsino whereas OSDF lepton configurations are formed by two isolated leptons, one originating from $\tilde{\Delta}^{--}$, the other from $\tilde{\Delta}^{++}$. To this end, SSSF leptons with small spatial separation qualify to be a direct indication of the doubly-charged Higgsinos in the spectrum (of the LRSUSY or of 3-3-1 model, for example). This feature is a clear-cut signal of extended SUSY models as it does not exist in the MSSM or in any of its extensions that contain only singly-charged fields.

In Figs. 5(a) and 5(b) we plot the binwise distributions of the transverse momenta of the final-state leptons for **S2** and **S3**, respectively. Since the same-sign leptons would be hard to distinguish based on their origin (from $\tilde{\Delta}$ or $\tilde{\ell}_i$) for **S2**, we prefer to plot the average transverse momentum of the same-flavor leptons. Theoretically, one expects leptons coming from the primary decay of $\tilde{\Delta}$ to be much harder than the ones coming from the intermediate slepton decay, $\tilde{\ell}_i^{\pm} \to \ell_i^{\pm} \tilde{\chi}_1^0$ for **S2**. The hardness of the leptons, when the $\tilde{\Delta}$ decays through the 2-body channel, is clearly dictated by the mass differences between the $\tilde{\Delta}$, the sleptons, and the LSP. Though this distinction is not possible at the LHC, one can understand the larger total cross section for **SPB**(**S3**) as compared to **SPB**(**S2**), because more soft leptons would be expected in the case of 2-body decays. Thus, the p_T cut on the charged leptons has a stronger effect on the signal for **SPB**(**S2**). A quick look at Fig. 5(a), where we plot the p_T for **S2** for both sample points, and 5 (b), which shows the distribution for **S3**, indicates that one finds more events at large p_T in Fig. 5(a) (2-body decay). This effect is due to the much harder leptons coming from the primary decay of the heavy $\tilde{\Delta}$.

In Fig. 6(a) and 6(b) we plot the binwise distributions of the invariant masses of the lepton pairs for **S2** and **S3**, respectively. These plots manifestly show differences between the SSSF and OSDF lepton pairs in regard to their invariant mass distributions. Indeed, the SSSF lepton pairs exhibit a sharp kinematic edge in their $M_{\ell\ell}$ distributions whereas the OSDF lepton pairs do not. The reason, also mentioned when discussing Fig. 4 above, is that SSSF lepton pairs originate from the cascade decay of the same $\tilde{\Delta}$. Since dilepton invariant mass does not change under boosts, this edge can be well-approximated for both **S2** and **S3** by the formula (in the rest frame of the decaying particle)

$$M_{\ell^{\pm}\ell^{\pm}}^{\max} = \sqrt{M_{\tilde{\Delta}}^2 + M_{\tilde{\chi}_1^0}^2 - 2M_{\tilde{\Delta}} E_{\tilde{\chi}_1^0}}, \tag{16}$$

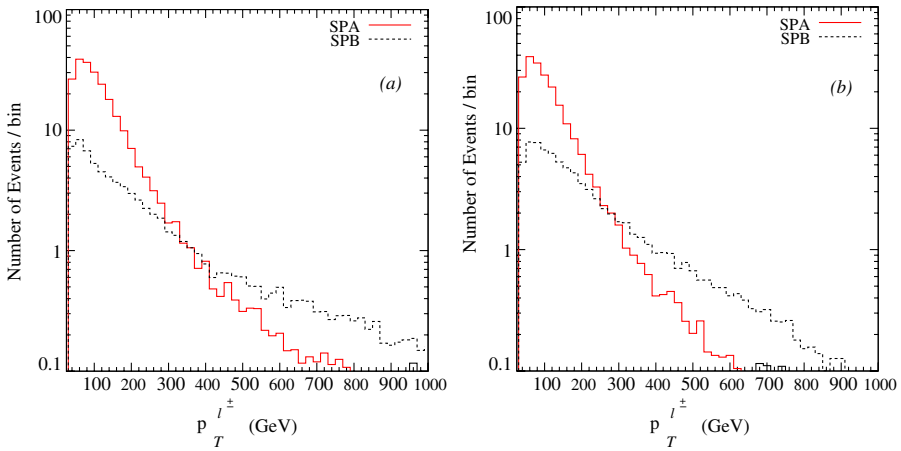

FIG. 5 (color online). Binwise distribution of transverse momenta p_T of the final-state leptons with binsize of 20 GeV and integrated luminosity of $\int \mathcal{L} dt = 30$ fb^{-1}. Panel (a) represents for 2-body (**S2**) decay whereas panel (b) stands for 3-body (**S3**) case.

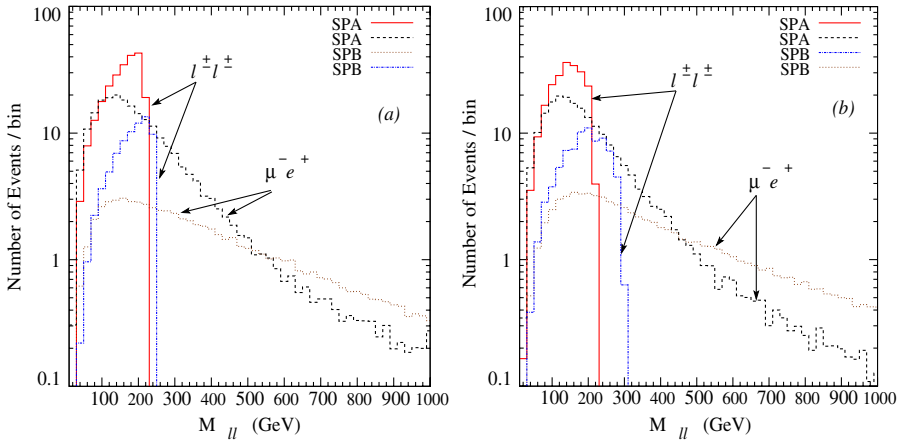

FIG. 6 (color online). Binwise invariant mass distribution of lepton pairs with binsize of 20 GeV and integrated luminosity of $\int \mathcal{L}dt = 30$ fb^{-1}. Panel (a) represents the 2-body (**S2**) case, and panel (b) does the 3-body (**S3**) case.

where $E_{\tilde{\chi}_1^0}$ is the energy of the LSP. This formula yields an edge in the invariant mass distribution of the SSSF lepton pairs at the bin around $M_{\ell^\pm\ell^\pm} = M_{\tilde{\Delta}} - M_{\tilde{\chi}_1^0}$ for both the **SPA** and **SPB** points in the case of the 3-body decay of $\tilde{\Delta}$ (**S3**), as can be seen in 6(b). This corresponds to the situation when the LSP is produced at rest in the frame of $\tilde{\Delta}$. For the case **S2** the situation is different, as the energy of the LSP also depends on the mass of the slepton when the $\tilde{\Delta}$ decays via on shell slepton (**S2**). In this case the invariant mass distribution of the SSSF lepton pairs exhibit an edge at a different bin compared to **S3**, as shown in Fig. 6(a) and its location is given by the formula

$$M_{\ell^\pm\ell^\pm}^{\max} = M_{\tilde{\Delta}}\sqrt{1-\left(\frac{m_{\tilde{\ell}}}{M_{\tilde{\Delta}}}\right)^2}\sqrt{1-\left(\frac{M_{\tilde{\chi}_1^0}}{m_{\tilde{\ell}}}\right)^2}. \qquad (17)$$

The edge in the SSSF dilepton invariant mass distribution yields a clear hint of a $\Delta L = 2$ interaction and a doubly-charged field in the underlying model of "new physics". The distributions of the OSDF dileptons exhibit no such edge at all since, in this case, the two leptons originate from the decays of the oppositely-charged, pair-produced $\tilde{\Delta}$'s.

In Fig. 7 we plot the binwise distribution of the missing transverse energy for all the cases under consideration. The heavier neutralinos in **SPB** yield more events at larger missing transverse energy, as expected.

B. Associated productions of doubly-charged Higgsinos and Charginos

In this section we study productions and decays of doubly-charged Higgsinos in association with the lightest chargino. The process under consideration, whose Feynman diagram is depicted in Fig. 2, has the form

$$pp \to \tilde{\Delta}^{--}\tilde{\chi}_1^+ \to (\ell_i^-\ell_i^-) + \ell_j^+ + \not{E}_T, \qquad (18)$$

where ℓ_i is not necessarily identical to ℓ_j. As mentioned above, this scattering process proceeds with the s-channel $W_{L,R}$ exchange, and yields invariably a trilepton signal, which has long been considered as a signal of SUSY, in general [22].

The cross section for singly-produced doubly-charged Higgsino turns out to be small at the sample points **SPA** and **SPB**, and hence, we devise a different benchmark point, **SPC**, to maximize single production of left-chirality doubly-charged Higgsinos. Sampling a wide region of LRSUSY parameter space, we could not find a significant region that enhances the single production of right-chirality doubly-charged Higgsino. In fact, a fine-grained

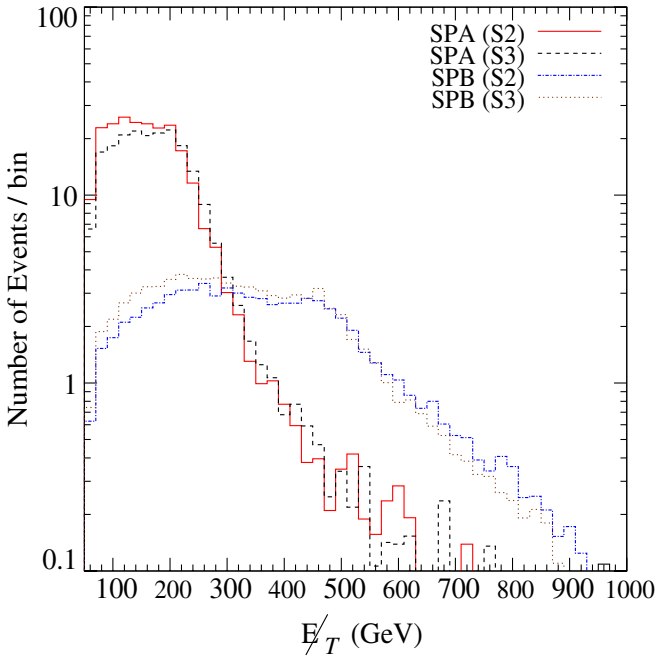

FIG. 7 (color online). Binwise distribution of the missing transverse energy of the signal with binsize of 20 GeV and integrated luminosity of $\int \mathcal{L}dt = 30$ fb^{-1}.

scan of the entire parameter space, with $M_{\tilde{\Delta}} = 300$ GeV, yields a maximal cross section for the right-chirality Higgsino which is still a factor of 3 smaller than that of the left-chirality Higgsino. They both become negligible around $M_{\tilde{\Delta}} = 300$ GeV since therein the composition of the lightest chargino changes abruptly. Consequently, in this section we use the sample point **SPC** and discuss the left-chirality doubly-charged Higgsino production in association with the lightest chargino $\tilde{\chi}_1^+$.

Figure 8 shows that, for all **SPC** parameter space with varying μ_3, the left-chirality doubly-charged Higgsino produced in association with the lightest chargino yields a large cross section for small Higgsino masses, and remains appreciable for doubly-charged Higgsinos as heavy as $M_{\tilde{\Delta}} \sim 450$ GeV. For the purpose of comparison, we also include the cross section for the right-chirality Higgsino, which starts dominating the cross section for the left-chirality one as $M_{\tilde{\Delta}}$ becomes larger than 450 GeV. One notes here that, since the chargino couplings to $\tilde{\Delta}_{L/R}$ depend on the entries in the mixing matrices of charginos, the input parameters in Table I play a crucial role in determining the production cross section. Since we assume $\mu_3 = 300$ GeV for **SPC**, the $3\ell + \not{E}_T$ signal comes from the decay of the left-chirality Higgsino only. The cross section for $pp \to \tilde{\Delta}_L^{--}\tilde{\chi}_1^+$ is around 30–40 fb for **SPC**. Based on further analysis the single-production cross section for **SPC** is quite stable against large variations in the other parameters of the model. Of course, this does not mean that the same holds for the signal cross section. For example, even though the $\tan\beta$ dependence of production cross section is very weak (as long as it does not significantly change the $\tilde{\Delta}_L^-$ composition of $\tilde{\chi}_1^+$), there is a stronger dependence in the decay modes, as can be seen from the couplings listed in the appendix.

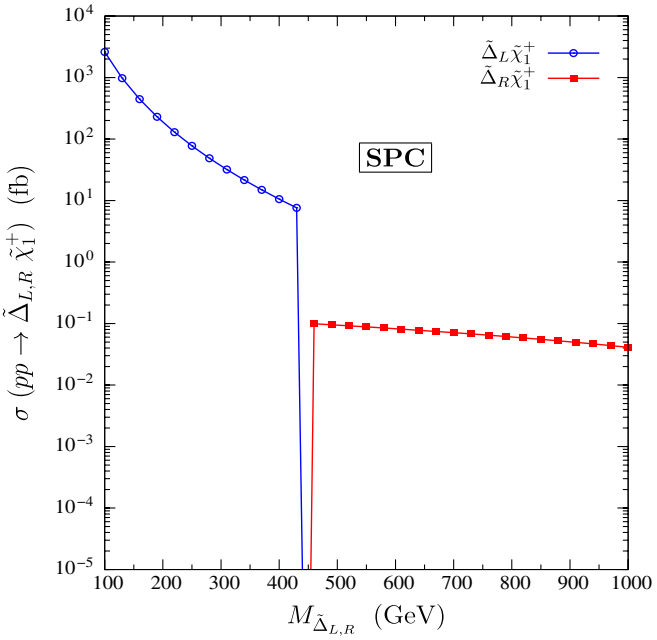

FIG. 8 (color online). The cross sections for associated productions of $\tilde{\Delta}_{L,R}$ and $\tilde{\chi}_1^\pm$ and in the LRSUSY model at LHC. The model parameters are as in **SPC** in Table I, except that $M_{\tilde{\Delta}^{--}} \equiv \mu_3$ is varied from 100 GeV up to 1 TeV.

As in pair-production, the $\tilde{\Delta}^{--}$ decays again into a pair of SSSF leptons and an LSP following Eq. (14), either through the 2-body decay mode (**S2**) or the 3-body decay mode (**S3**). The three possible chargino decay modes are depicted in Fig. 2. We find that the chargino has almost 100% branching ratio to a neutrino and slepton for **SPC**. Then sleptons decay as in Eq. (14). This gives a $3\ell + \not{E}_T$ final state where the missing transverse energy is due to an undetected LSP and the neutrino. For the benchmark point **SPC** the signal gets all the contribution from the left-chirality state.

The single $\tilde{\Delta}^{--}$ production gives rise to a trilepton signal at the LHC experiments. In the numerical analysis, following the same notation and same kinematic cuts as in the previous subsection, we illustrate the case where $\ell_i = \mu$ and $\ell_j = e$. Thus, we know that the e^+ always comes from the chargino while the same-sign muons originate from the doubly-charged Higgsino.

The production cross section for the sample point **SPC** is:

(1) **SPC**:

$$\sigma(\tilde{\Delta}_L^{--}\tilde{\chi}_1^+) = 36.57 \text{ fb},$$

and after imposing the kinematic cuts, the total signal cross section becomes

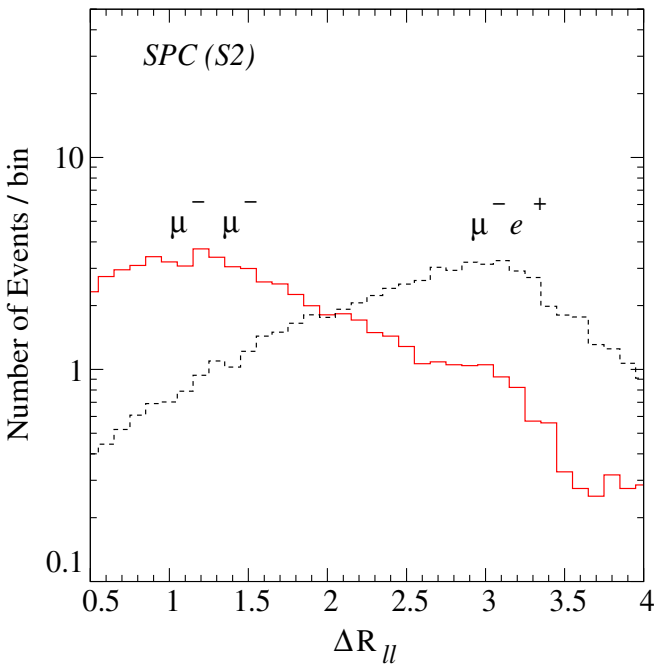

FIG. 9 (color online). Binwise distribution of ΔR with 0.1 and integrated luminosity of $\int \mathcal{L}dt = 30$ fb^{-1}.

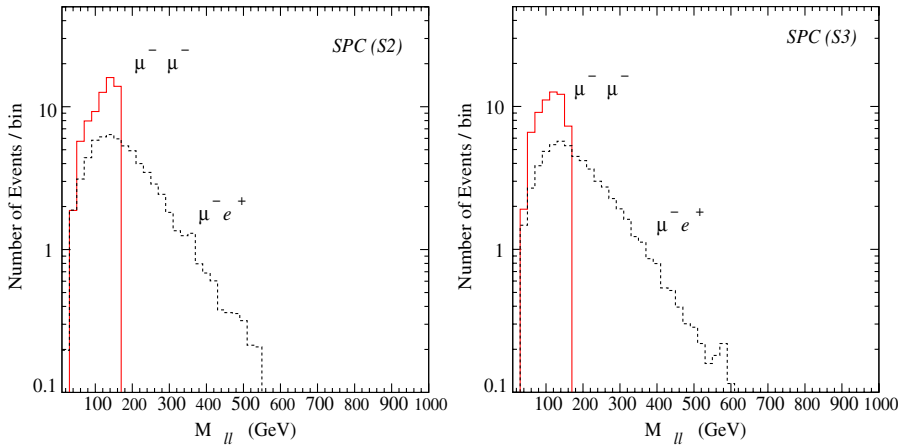

FIG. 10 (color online). Binwise invariant mass distribution of a pair of leptons in the final state with binsize 20 GeV and integrated luminosity of $\int \mathcal{L}dt = 30$ fb^{-1}.

(a) **S2** $\sigma(2\ell_i^-\ell_j^+\not{E}_T) = 2.24$ fb,
(b) **S3** $\sigma(2\ell_i^-\ell_j^+\not{E}_T) = 2.03$ fb,

where $\ell_i = \mu$ and $\ell_j = e$. These numerical estimates hold for the specific choice for the final state, i.e. $2\mu^- + e^+ + \not{E}_T$.

In parallel to the analysis of $4\ell + \not{E}_T$ signal in the previous subsection, we here plot various distributions in Figs. 9–13 by considering specifically $2\ell_i^- + \ell_j^+ + \not{E}_T$ signal with $\ell_i = \mu$ and $\ell_j = e$. Several features observed in these figures have already been covered by discussions in the previous subsection. In particular, the distributions of the SSSF leptons are quite similar to the ones for the $4\ell + \not{E}_T$ signal. This is actually expected since SSSF leptons are exclusively generated by decays of the doubly-charged Higgsino, a common feature for both tetralepton and trilepton final states. Compared to the $4\ell + \not{E}_T$ signal, however, distributions for OSDF leptons are slightly different since the oppositely-charged electron comes exclusively from selectron decay and possesses different kinematics. For example, as compared to the $4\ell + \not{E}_T$ signal, there are fewer events at large missing energy and also at large transverse momentum, for the electron from the chargino decay as well as the muons from the doubly-charged Higgsino decay. This stems from the fact that the final

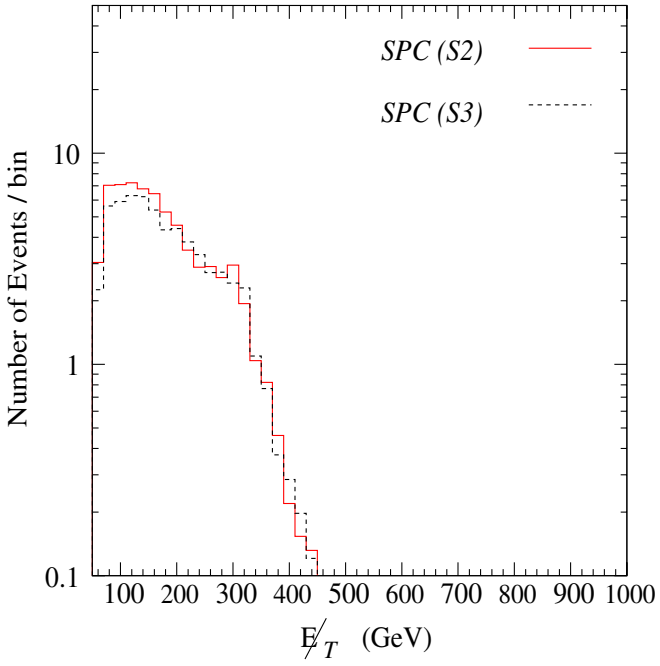

FIG. 11 (color online). Binwise distribution of missing transverse energy for the signal with binsize 20 GeV and integrated luminosity of $\int \mathcal{L}dt = 30$ fb^{-1}.

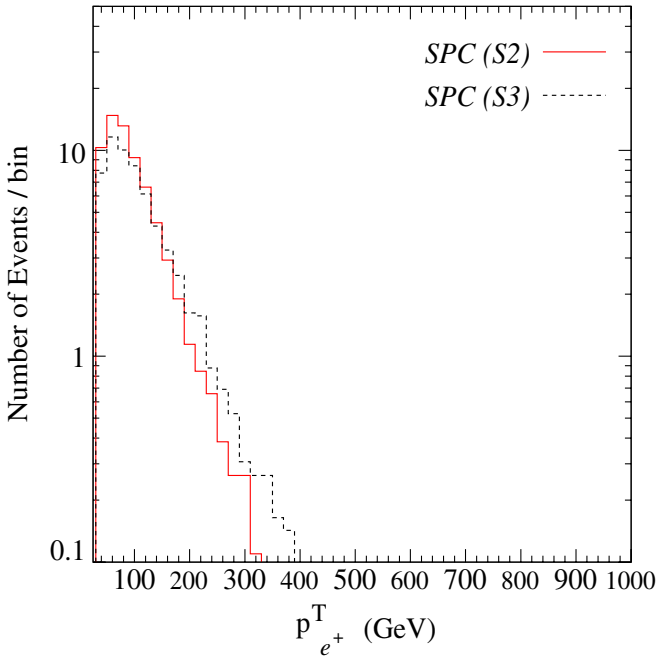

FIG. 12 (color online). Binwise distribution of transverse momentum of e^+ with binsize is 20 GeV and integrated luminosity of $\int \mathcal{L}dt = 30$ fb^{-1}.

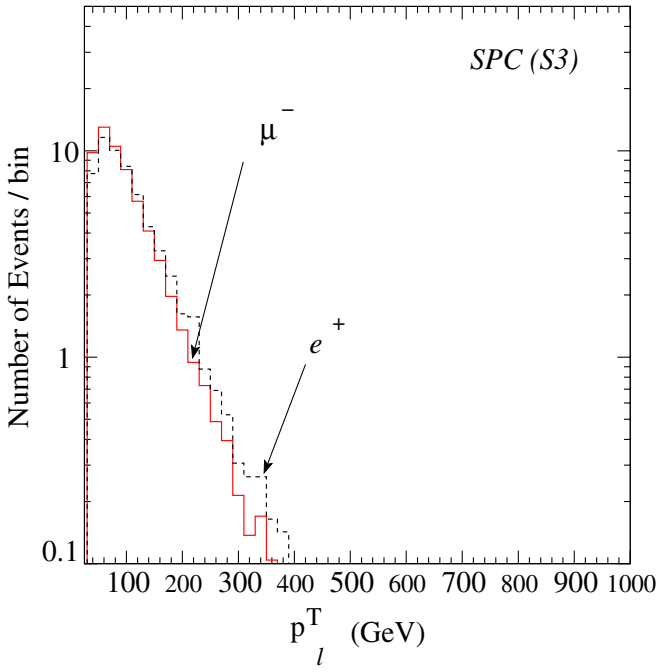

FIG. 13 (color online). Binwise distribution of transverse momentum of leptons for the 3-body cases with binsize is 20 GeV and integrated luminosity of $\int \mathcal{L} dt = 30$ fb^{-1}.

leptons are soft kinematically. It is also seen from the figures that the distributions for **S2** and **S3** are similar since the mass splitting $M_{\tilde{\Delta}} - M_{\tilde{l}} \sim 85$ GeV is comparable to $M_{\tilde{l}} - M_{\tilde{\chi}^0} \sim 72$ GeV.

IV. DISCUSSION AND CONCLUSION

We have studied the LHC signals of doubly-charged Higgsinos present in extended SUSY models such as the LRSUSY. The doubly-charged Higgs fermions in the spectrum are a characteristic feature of LRSUSY which can directly and unambiguously distinguish the model from the MSSM [and its various extensions like NMSSM and $U(1)'$ models] by measuring certain leptonic events. We have given a detailed account of the leptonic signals originating from production and decay of (i) doubly-charged Higgsino pairs and of (ii) single doubly-charged Higgsino plus chargino . For the production mode (i) the leptonic final state invariably involves $(\ell_i^- \ell_i^-) + (\ell_j^+ \ell_j^+) + \not{E}_T$, that is, a pair of SSSF dileptons plus missing energy taken away by the LSP, $\tilde{\chi}_1^0$. On the other hand, for (ii) the leptonic final state is composed of $(\ell_i^- \ell_i^-) + \ell_j^+ + \not{E}_T$, that is, a trilepton signal. Our simulation studies yield rather generally, for $\ell_i \neq \ell_j$, that the SSSF dileptons exhibit (a) a narrow spatial extension and (b) a sharp edge in dilepton invariant mass, in contrast to OSDF dileptons. There are additional distinctive features which become visible via transverse momentum/energy distributions. These "experimental" results provide a testing ground for an attempt to determine the underlying SUSY model at the TeV scale.

For a clearer view of the distinguishing power of these features, it proves useful to compare them with expectations of another SUSY model such as the MSSM. Concerning the tetralepton signal $(\ell_i^- \ell_i^-) + (\ell_j^+ \ell_j^+) + \not{E}_T$ in LRSUSY, one notes that a similar signal also arises in the MSSM via pair-production-and-decay of the next-to-lightest neutralino $\tilde{\chi}_2^0$ (which is dominated by λ_Z at least in minimal supergravity) with a different topology $(\ell_i^- \ell_i^+) + (\ell_j^- \ell_j^+) + \not{E}_T$ [23]. Therefore, in contrast to leptons originating from decays of doubly-charged Higgsinos whose spatial distributions are shown in Fig. 4, in the MSSM OSSF dileptons are expected to have a narrow spatial extension. This and other features, which follow from the plots in the previous section, enable one to distinguish between LRSUSY and MSSM in tetralepton signals.

Concerning the trilepton signal $(\ell_i^- \ell_i^-) + \ell_j^+ + \not{E}_T$, one notices that a similar signal, $(\ell_i^- \ell_i^+) + \ell_j^+ + \not{E}_T$, also arises in the MSSM via associated productions χ_2^0 and $\tilde{\chi}_1^+$, and their subsequent decays into leptons and $\tilde{\chi}_1^0$. As in the tetralepton case, the two models predict different topologies for final-state leptons. The $\tilde{\chi}_2^0$ decay gives rise to OSSF leptons and in contrast to LRSUSY expectation depicted in Fig. 9, in the MSSM OSSF leptons are expected to have a narrow spatial extension. The trilepton signal with missing transverse energy has long been identified as one of the most promising signals of SUSY [22] in general. Here we see how it can be used to test for a different scenario than MSSM.

This procedure of discriminating different models of "new physics" with lepton spectrum naturally extends to other models, not necessarily of supersymmetric nature. For example, in universal extra dimensions (UED), pair-production of two excited Z bosons—the first Kaluza-Klein (KK) level Z_1—invariably leads to tetralepton signals through the cascade decay of each Z_1 (with LKP being the lightest KK particle whose stability is guaranteed by the KK symmetry) [24]. By the same token, the trilepton signal follows from the associated production of charged and neutral gauge bosons, $W_1^\pm Z_1$, and their subsequent decays into leptons and LKP. In terms of the event topologies, trilepton and tetralepton signals of UED are similar to those of the MSSM, and thus, distinguishing UED from LRSUSY is accomplished with the same strategy used for the MSSM.

Also interesting are models with low-scale $U(1)_{B-L}$ invariance, which accommodate a light right-handed Majorana neutrino N [25]. The pair-produced right-handed neutrinos can give rise to the tetralepton signal via $N \to \ell_i^+ W^- \to \ell_i^+ \ell_j^- \bar{\nu}_j$ decay. The trilepton signal can come from associated $\ell_i N$ production and is strongly suppressed. The LHC signatures of this model are similar to those of the MSSM and UED, and SSSF lepton distributions enable one to distinguish it from LRSUSY [26].

These case studies can be extended to a multitude of "new physics" models at both qualitative and quantitative

level. In each case, LRSUSY, whose spectrum consists of doubly-charged Higgsinos, is found to differ from the rest by having SSSF proximate dileptons at the final state. Our results show convincingly clear that doubly-charged Higgsinos give rise to rather special leptonic events at the LHC, making them firmly distinguishable from other SUSY particles and also from particles in several other models of physics at the TeV scale.

ACKNOWLEDGMENTS

The work of M. F. and I. T. is supported in part by NSERC of Canada under the Grant No. SAP01105354. The work of D. D. was supported by Alexander von Humboldt-Stiftung Friedrich Wilhelm Bessel-Forschungspreise and by the Turkish Academy of Sciences via the GEBIP grant. K. H. and S. K. R. gratefully acknowledge the support from the Academy of Finland (Project No. 115032). We would like to thank M. T. Ataol and P. M. K. Ravuri for useful technical discussions about CALCHEP package, A. Belyaev for discussions on CALCHEP-PYTHIA interface, R. Kinnunen and S. Raychaudhuri for discussions, and Goran Senjanović for enlightening email exchanges.

APPENDIX

In this appendix we list down all the Feynman rules necessary for analyzing productions and decays of doubly-charged Higgsinos in the LRSUSY model.

Scalar-Scalar-Z Boson, γ:

(i) $A^\mu \tilde{q}\tilde{q}^\star$: $-ieQ_q(p_q + p_{q^*})^\mu$

(ii) $Z_L^\mu \tilde{q}\tilde{q}^\star$: $-i\frac{g_L}{\cos\theta_W}(T_{3q}^L - Q_f \sin^2\theta_W)(p_q + p_{q^*})^\mu$

(iii) $Z_R^\mu \tilde{q}\tilde{q}^\star$: $-i\frac{g_R\sqrt{\cos 2\theta_W}}{\cos\theta_W}(T_{3q}^R - \frac{1}{6}\frac{\sin^2\theta_W}{\cos 2\theta_W})(p_q + p_{q^*})^\mu$

Scalar-Scalar-W bosons:

(i) $W_L^\mu \tilde{l}_L \tilde{\nu}_L$: $-i\frac{g_L}{\sqrt{2}}(p_l + p_\nu)^\mu$

(ii) $W_R^\mu \tilde{l}_R \tilde{\nu}_R$: $-i\frac{g_R}{\sqrt{2}}(p_l + p_\upsilon)^\mu$

Fermion-Fermion-W bosons:

(i) $W_L^\mu l\bar{\nu}$: $-i\frac{g_L}{\sqrt{2}}\gamma^\mu P_L$

(ii) $W_R^\mu l\bar{\nu}$: $-i\frac{g_R}{\sqrt{2}}\gamma^\mu P_R$

(iii) $W_L^\mu q\bar{q}'$: $-i\frac{g_L}{\sqrt{2}}\gamma^\mu P_L$

(iv) $W_R^\mu q\bar{q}'$: $-i\frac{g_R}{\sqrt{2}}\gamma^\mu P_R$

(v) $W_L^\mu \tilde{\chi}_k^+ \tilde{\Delta}_L^{--}$: $ig_L\gamma^\mu(V_{k5}^\star P_L + U_{k5}P_R)$

(vi) $W_R^\mu \tilde{\chi}_k^+ \tilde{\Delta}_R^{--}$: $ig_R\gamma^\mu(V_{k6}^\star P_L + U_{k6}P_R)$

(vii) $W_L^\mu \tilde{\chi}_k^+ \tilde{\chi}_j^0$: $-ig_L\gamma^\mu(L_{jk}^L P_L + L_{jk}^R P_R)$

(viii) $W_R^\mu \tilde{\chi}_k^+ \tilde{\chi}_j^0$: $-ig_R\gamma^\mu(R_{jk}^L P_L + R_{jk}^R P_R)$ with the matrix elements given in terms of chargino and neutralino mixing matrices as

$$
\begin{aligned}
L_{jk}^L &= -N_{k1}^\star V_{j1} + \frac{1}{\sqrt{2}}N_{k5}^\star V_{j4} + N_{k6}^\star V_{j5} \\
&\quad + \frac{1}{\sqrt{2}}N_{k11}^\star V_{j3} \\
L_{jk}^R &= -U_{j1}^\star N_{k1} - \frac{1}{\sqrt{2}}U_{j4}^\star N_{k4} + N_{k7}^\star V_{j5} \\
&\quad - \frac{1}{\sqrt{2}}U_{j4}^\star N_{k10} \\
R_{jk}^L &= -N_{k2}^\star V_{j2} + \frac{1}{\sqrt{2}}N_{k5}^\star V_{j4} + N_{k8}^\star V_{j6} \\
&\quad + \frac{1}{\sqrt{2}}N_{k11}^\star V_{j3} \\
R_{jk}^R &= -U_{j2}^\star N_{k2} - \frac{1}{\sqrt{2}}U_{j3}^\star N_{k4} + U_{j6}^\star N_{k9} \\
&\quad - \frac{1}{\sqrt{2}}U_{j4}^\star N_{k10}
\end{aligned}
$$

Fermion-Fermion-Z Boson, γ:

(i) $\gamma^\mu \tilde{\Delta}_{L,R}^{--}\bar{\tilde{\Delta}}_{L,R}^{--}$: $2ie\gamma^\mu$

(ii) $Z_L^\mu \tilde{\Delta}_L^{--}\bar{\tilde{\Delta}}_L^{--}$: $i\frac{g_L\cos 2\theta_W}{\cos\theta_W}\gamma^\mu$

(iii) $Z_L^\mu \tilde{\Delta}_R^{--}\bar{\tilde{\Delta}}_R^{--}$: $-i\frac{2g_L\sin^2\theta_W}{\cos\theta_W}\gamma^\mu$

(iv) $Z_R^\mu \tilde{\Delta}_L^{--}\bar{\tilde{\Delta}}_L^{--}$: $i\frac{g_L\sqrt{\cos 2\theta_W}}{\cos\theta_W}\gamma^\mu$

(v) $Z_R^\mu \tilde{\Delta}_R^{--}\bar{\tilde{\Delta}}_R^{--}$: $-i\frac{g_L(1-3\sin^2\theta_W)}{\cos\theta_W\sqrt{\cos 2\theta_W}}\gamma^\mu$

Fermion-Fermion-Scalar Fermion:

(i) $\tilde{\Delta}_L^{--}\tilde{l}l$: $-2h_{ll}\mathcal{C}^{-1}P_L$

(ii) $\tilde{\Delta}_R^{--}\tilde{l}l$: $-2h_{ll}\mathcal{C}^{-1}P_R$

(iii) $\tilde{\Delta}_L^{-}\tilde{l}\nu$: $h_{ll}\mathcal{C}^{-1}P_L$

(iv) $\tilde{\Delta}_L^{-}l\tilde{\nu}$: $h_{ll}\mathcal{C}^{-1}P_L$

(v) $\tilde{\Delta}_R^{-}\tilde{l}\nu$: $h_{ll}\mathcal{C}^{-1}P_R$

(vi) $\tilde{\Delta}_R^{-}l\tilde{\nu}$: $h_{ll}\mathcal{C}^{-1}P_R$

(vii) $\tilde{\chi}_k^0\tilde{l}\,\bar{l}$: $-i\{[\sqrt{2}g_L(\frac{1}{2}N_{k1} - \frac{1}{2}(\frac{\cos 2\theta_W}{\cos^2\theta_W} + \tan^2\theta_W)N_{k2} - \frac{\sin\theta_W\sqrt{\cos 2\theta_W}}{\cos^2\theta_W}N_{k3} + \frac{m_l}{2M_W\cos\beta}N_{k5})]P_L - [\sqrt{2}g_R((\frac{\cos 2\theta_W}{2\cos^2\theta_W} - \tan^2\theta_W)N_{k2} - \frac{\sin\theta_W\sqrt{\cos 2\theta_W}}{\cos^2\theta_W}N_{k3} + \frac{m_l}{2M_W\cos\beta}N_{k5}^\star)]P_R\}$

(viii) $\tilde{\chi}_k^0\tilde{\nu}\,\bar{\nu}$: $-i\{[\sqrt{2}g_L(\frac{1}{2}N_{k1} + \frac{1}{2}(\frac{\cos 2\theta_W}{\cos^2\theta_W} - \tan^2\theta_W)N_{k2} - \frac{\sin\theta_W\sqrt{\cos 2\theta_W}}{\cos^2\theta_W}N_{k3} + \frac{m_l}{2M_W\cos\beta}N_{k5})]P_L - [\sqrt{2}g_R(\frac{\cos 2\theta_W}{2\cos^2\theta_W}N_{k2} - \frac{\sin\theta_W\sqrt{\cos 2\theta_W}}{2\cos^2\theta_W}N_{k3} + \frac{m_l}{2M_W\cos\beta}N_{k5}^\star)]P_R\}$

[1] D. A. Demir, M. Frank, and I. Turan, Phys. Rev. D **73**, 115001 (2006).

[2] L. Pape and D. Treille, Rep. Prog. Phys. **69**, 2843 (2006); M. Spiropulu, arXiv:0801.0318.

[3] S. Cecotti, J. P. Derendinger, S. Ferrara, L. Girardello, and M. Roncadelli, Phys. Lett. **156B**, 318 (1985); J. D. Breit, B. A. Ovrut, and G. C. Segre, Phys. Lett. **158B**, 33 (1985); J. L. Hewett and T. G. Rizzo, Phys. Rep. **183**, 193 (1989); M. Cvetic and P. Langacker, Phys. Rev. D **54**, 3570 (1996).

[4] M. Cvetič and J. Pati, Phys. Lett. **135B**, 57 (1984); R. N. Mohapatra and A. Rašin, Phys. Rev. D **54**, 5835 (1996); R. Kuchimanchi, Phys. Rev. Lett. **76**, 3486 (1996); R. N. Mohapatra, A. Rašin, and G. Senjanović, Phys. Rev. Lett. **79**, 4744 (1997); C. S. Aulakh, K. Benakli, and G. Senjanović, Phys. Rev. Lett. **79**, 2188 (1997); C. S. Aulakh, A. Melfo, and G. Senjanović, Phys. Rev. D **57**, 4174 (1998).

[5] R. M. Francis, M. Frank, and C. S. Kalman, Phys. Rev. D **43**, 2369 (1991); K. Huitu, J. Maalampi, and M. Raidal, Phys. Lett. B **328**, 60 (1994); K. Huitu, J. Maalampi, and M. Raidal, Nucl. Phys. **B420**, 449 (1994); K. Huitu and J. Maalampi, Phys. Lett. B **344**, 217 (1995).

[6] R. N. Mohapatra and A. Rasin, Phys. Rev. Lett. **76**, 3490 (1996); Phys. Rev. D **54**, 5835 (1996); R. Kuchimanchi, Phys. Rev. Lett. **76**, 3486 (1996).

[7] R. N. Mohapatra and G. Senjanovic, Phys. Rev. Lett. **44**, 912 (1980); Phys. Rev. D **23**, 165 (1981); M. Gell-Mann, P. Ramond, and R. Slansky, in *Supergravity*, edited by P. van Nieuwenhuizen *et al.* (North Holland, Amsterdam, 1980), p. 315; T. Yanagida, in *Proceedings of the Workshop on the Unified Theory and the Baryon Number in the Universe*, edited by O. Sawada and A. Sugamoto (KEK, Tsukuba, Japan, 1979), p. 95; S. L. Glashow, in *Proceedings of the Summer Institute on Quarks and Leptons*, edited by M. Levy *et al.* (Plenum Press, New York, 1980), p. 687.

[8] C. S. Aulakh, A. Melfo, A. Rasin, and G. Senjanovic, Phys. Rev. D **58**, 115007 (1998).

[9] C. S. Aulakh, A. Melfo, and G. Senjanovic, Phys. Rev. D **57**, 4174 (1998).

[10] Z. Chacko and R. N. Mohapatra, Phys. Rev. D **58**, 015003 (1998); B. Dutta and R. N. Mohapatra, Phys. Rev. D **59**, 015018 (1998).

[11] K. Huitu, J. Maalampi, and M. Raidal, Report No. HU-SEFT-I-1995-1, 1995 (unpublished); M. Frank, Phys. Rev. D **62**, 053004 (2000).

[12] M. Raidal and P. M. Zerwas, Eur. Phys. J. C **8**, 479 (1999).

[13] M. Frank, K. Huitu, and S. K. Rai, Phys. Rev. D **77**, 015006 (2008).

[14] M. Singer, J. W. F. Valle, and J. Schechter, Phys. Rev. D **22**, 738 (1980); P. H. Frampton, Phys. Rev. Lett. **69**, 2889 (1992); J. C. Montero, F. Pisano, and V. Pleitez, Phys. Rev. D **47**, 2918 (1993); R. Foot, O. F. Hernandez, F. Pisano, and V. Pleitez, Phys. Rev. D **47**, 4158 (1993); R. Foot, H. N. Long, and T. A. Tran, Phys. Rev. D **50**, R34 (1994); H. N. Long, Phys. Rev. D **54**, 4691 (1996).

[15] M. Frank, Phys. Lett. B **540**, 269 (2002).

[16] C. S. Aulakh, B. Bajc, A. Melfo, A. Rasin, and G. Senjanovic, Phys. Lett. B **460**, 325 (1999).

[17] H. Georgi and M. Machacek, Nucl. Phys. **B262**, 463 (1985); K. Huitu, J. Maalampi, A. Pietila, and M. Raidal, Nucl. Phys. **B487**, 27 (1997); K. Huitu, P. N. Pandita, and K. Puolamaki, Phys. Lett. B **415**, 156 (1997); K. Huitu, P. N. Pandita, and K. Puolamaki, Phys. Lett. B **423**, 97 (1998); S. Chakrabarti, D. Choudhury, R. M. Godbole, and B. Mukhopadhyaya, Phys. Lett. B **434**, 347 (1998); K. Huitu, P. N. Pandita, and K. Puolamaki, arXiv:hep-ph/9904388; S. Godfrey, P. Kalyniak, and N. Romanenko, Phys. Rev. D **65**, 033009 (2002); J. Maalampi and N. Romanenko, Phys. Lett. B **532**, 202 (2002); S. Godfrey, P. Kalyniak, and N. Romanenko, Phys. Lett. B **545**, 361 (2002); A. G. Akeroyd and M. Aoki, Phys. Rev. D **72**, 035011 (2005); B. Mukhopadhyaya and S. K. Rai, Phys. Lett. B **633**, 519 (2006); J. E. Cieza Montalvo, N. V. Cortez, J. Sa Borges, and M. D. Tonasse, Nucl. Phys. **B756**, 1 (2006); **B796**, 422 (E) (2008); G. Azuelos, K. Benslama, and J. Ferland, J. Phys. G **32**, 73 (2006); T. Rommerskirchen and T. Hebbeker, J. Phys. G **34**, N47 (2007).

[18] J. Abdallah *et al.* (DELPHI Collaboration), Phys. Lett. B **552**, 127 (2003); G. Abbiendi *et al.* (OPAL Collaboration), Phys. Lett. B **577**, 93 (2003); P. Achard *et al.* (L3 Collaboration), Phys. Lett. B **576**, 18 (2003); D. E. Acosta *et al.* (CDF Collaboration), Phys. Rev. Lett. **93**, 221802 (2004); **95**, 071801 (2005); T. Aaltonen (CDF Collaboration), FERMILAB Report No. FERMILAB-PUB-07-709-E (unpublished).

[19] A. Pukhov, arXiv:hep-ph/0412191.

[20] T. Sjostrand, S. Mrenna, and P. Skands, J. High Energy Phys. 05 (2006) 026.

[21] J. Pumplin, D. R. Stump, J. Huston, H. L. Lai, P. Nadolsky, and W. K. Tung, J. High Energy Phys. 07 (2002) 012; D. Stump, J. Huston, J. Pumplin, W. K. Tung, H. L. Lai, S. Kuhlmann, and J. F. Owens, J. High Energy Phys. 10 (2003) 046; T. Sjostrand, S. Mrenna, and P. Skands, J. High Energy Phys. 05 (2006) 026.

[22] H. Baer, K. Hagiwara, and X. Tata, Phys. Rev. D **35**, 1598 (1987); P. Nath and R. Arnowitt, Mod. Phys. Lett. A **2**, 331 (1987); H. Baer and X. Tata, Phys. Rev. D **47**, 2739 (1993); H. Baer, C. h. Chen, F. Paige, and X. Tata, Phys. Rev. D **50**, 4508 (1994); B. Abbott *et al.* (D0 Collaboration), Phys. Rev. Lett. **80**, 1591 (1998); F. Abe *et al.* (CDF Collaboration), Phys. Rev. Lett. **80**, 5275 (1998); V. D. Barger, C. Kao, and T. j. Li, Phys. Lett. B **433**, 328 (1998).

[23] H. Baer, X. Tata, and J. Woodside, Phys. Rev. D **45**, 142 (1992); S. Abdullin *et al.* (CMS Collaboration), J. Phys. G **28**, 469 (2002); A. J. Barr, CERN, Report No. CERN-THESIS-2004-002, 2002.

[24] H. C. Cheng, K. T. Matchev, and M. Schmaltz, Phys. Rev. D **66**, 056006 (2002).

[25] S. Khalil, J. Phys. G **35**, 055001 (2008); M. Abbas and S. Khalil, J. High Energy Phys. 04 (2008) 056.

[26] K. Huitu, S. Khalil, H. Okada, and S. K. Rai, arXiv:0803.2799.